2014

Brain network markers of abnormal cerebral glucose metabolism and blood flow in Parkinson's disease

S. C. Peng
Northwell Health

D. Eidelberg
Hofstra Northwell School of Medicine

Y. L. Ma
Northwell Health

HHS Public Access

Author manuscript

Neurosci Bull. Author manuscript; available in PMC 2015 September 01.

Published in final edited form as:

Neurosci Bull. 2014 October ; 30(5): 823–837. doi:10.1007/s12264-014-1472-x.

Brain network markers of abnormal cerebral glucose metabolism and blood flow in Parkinson's disease

Shichun Peng, **David Eidelberg**, and **Yilong Ma**

Center for Neurosciences, The Feinstein Institute for Medical Research, North Shore-Long Island Jewish Health System, Manhasset, New York, USA

Abstract

Neuroimaging of cerebral glucose metabolism and blood flow is ideally suited to assay widely-distributed brain circuits as a result of local molecular events and behavioral modulation in the central nervous system. With the progress in novel analytical methodology, this endeavor has succeeded in unraveling the mechanisms underlying a wide spectrum of neurodegenerative diseases. In particular, statistical brain mapping studies have made significant strides in describing the pathophysiology of Parkinson's disease (PD) and related disorders by providing signature biomarkers to determine the systemic abnormalities in brain function and evaluate disease progression, therapeutic responses, and clinical correlates in patients. In this article, we review the relevant clinical applications in patients in relation to healthy volunteers with a focus on the generation of unique spatial covariance patterns associated with the motor and cognitive symptoms underlying PD. These characteristic biomarkers can be potentially used not only to improve patient recruitment but also to predict outcomes in clinical trials.

Keywords

Parkinson's disease; metabolism; blood flow; PET; SPECT; movement disorder; network analysis; imaging biomarkers

Introduction

Functional brain imaging with positron emission tomography (PET) and single-photon emission computed tomography (SPECT) has provided novel insights into the pathophysiology of Parkinson's disease (PD) and related movement disorders. The integrity of the presynaptic nigrostriatal dopaminergic systems can be evaluated by measuring the dopamine storage capacity using [^{18}F] fluorodopa (FDOPA), or dopamine transporter (DAT) binding using radiotracers such as [^{123}I]βCIT and [^{18}F]FPCIT (see reviews [1, 2]). Postsynaptic dopamine receptor systems can be assayed with radioligands that bind specifically to D_1 or D_2 receptors. In addition, PET has been used to study regional neuronal activity by quantifying resting-state regional cerebral glucose metabolism (rCMRglc) with [^{18}F]fluorodeoxyglucose (FDG)[3] and regional cerebral blood flow (rCBF) activation responses with [^{15}O]H_2O[4]. Abnormal rCBF distributions in the resting state can also be

Corresponding author: Yilong Ma. yma@nshs.edu.

measured using PET and SPECT perfusion tracers. In particular, imaging of cerebral metabolism and blood flow has contributed greatly to the understanding of the abnormal brain circuitry underlying the pathophysiology of PD.

PET/SPECT can be particularly useful in assessing the consequences of nigrostriatal dopamine deficiency on the functional networks of the basal ganglia. Although the primary pathological abnormality in PD is located in the substantia nigra, the degeneration of dopaminergic projection neurons to the striatum leads to widespread changes in the functional activity of the basal ganglia[5]. Specifically, the loss of inhibitory dopaminergic input to the striatum increases the inhibitory output from the putamen to the external globus pallidus (GPe), decreases the inhibitory output from the GPe to the subthalamic nucleus (STN), and causes functional over-activity of the STN and internal globus pallidus (GPi), resulting in reduced output from the ventrolateral thalamus to the cortex. This classic model has been modified to emphasize the cognitive dysfunction associated with PD[6] and is linked to concurrent changes in regional glucose metabolism and blood flow.

We review the advances in functional brain imaging studies of PD in the resting state based on analyses of rCMRglc and rCBF in patients and healthy volunteers. As in most neurodegenerative conditions, these two variables are considered to be coupled in PD and related to synaptic activity at the regional level. We also summarize the use of novel analytical techniques in the clinical diagnosis and evaluation of PD. These include both univariate and multivariate statistical approaches such as statistical parametric mapping (SPM) and principal component analysis (PCA) for volume of interest (VOI) or voxel-wise analysis over the whole brain. In addition, we focus on the application of these imaging methods to the selection of suitable candidates for surgical trials and the assessment of their treatment outcome.

Functional Brain Imaging: Univariate Analyses

PET/SPECT imaging of rCMRglc and rCBF has been used extensively to identify changes in regional brain function in patients with PD comparable to those revealed in experimental animal models[7, 8]. The bulk of this effort is based on the use of SPM to localize regionally specific differences and functional-clinical correlates in PD patients scanned when they are off dopaminergic medications. Functional brain images are spatially transformed into a standard anatomical space to allow mapping analysis on a voxel basis. To reduce inter-individual variability in anatomical and functional substrates, images are usually ratio-normalized to a global mean or other reference value that is assumed to be preserved in the diseased brain. Consequently, only relative measures of functional brain activity are used in most studies.

Cerebral Metabolism Studies

Because the local rate of glucose metabolism is a direct marker of synaptic activity, PET with FDG has been the most common approach to studying abnormal brain function in PD. By using FDG PET images from multiple cohorts of patients and healthy controls we and other researchers have reported a reproducible pattern of abnormal regional metabolism in PD (Fig. 1) characterized bilaterally by increases in the putamen, thalamus, cerebellum,

pons, and sensorimotor cortex (SMC), and decreases in the lateral frontal and parieto-occipital areas[9–11]. This is in accordance with a dual-tracer PET study with both FDG and [^{15}O]O_2 showing bilaterally increased energy metabolism in the putamen and pallidum in early unmedicated PD patients[12]. Regional metabolism in the cerebellum is also elevated in early-stage and advanced PD patients[13, 14], suggesting that cerebellar hypermetabolic activity in PD is closely linked to akinesia and rigidity but not to tremor. It has been further reported that clinical scores of motor symptoms are correlated positively with rCMRglc in the bilateral putamen and pallidum[15], and in the midbrain, cerebellum, and motor cortex[16]. These reports indicate a pathophysiologic association between subcortical hypermetabolism and motor dysfunction in PD.

Unique features of cortical hypometabolism in PD have also been frequently reported. An early study reported pronounced occipital hypometabolism in the more severely affected hemisphere in PD[17]. The asymmetry in this metabolic reduction correlated inversely with finger-tapping performance in a subset of patients with more unilateral motor impairment. While hypometabolism is limited in the frontal and occipital cortices of PD patients with no cognitive impairment[18], it becomes more widespread within cortical regions in advanced PD[14]. Further, the relationships of abnormal rCMRglc with clinical symptoms and impaired striatal DAT binding have been examined in *de novo* untreated PD patients[19]. Correlation analyses showed that the UPDRS motor ratings were negatively correlated with rCMRglc in the premotor cortex (PMC), while putaminal DAT binding was positively correlated with rCMRglc in the premotor, dorsolateral prefrontal, anterior prefrontal, and orbitofrontal cortices. This method also led to a set of disease-related brain templates for PD and atypical PD to aid single-case differential diagnosis[10, 11]. These results may represent the cortical functional correlates of nigrostriatal dysfunction in the motor basal ganglia-cortical circuitry in parkinsonism.

FDG PET has also been used to delineate the metabolic functional correlates of PD with cognitive impairment. Regional metabolism is markedly reduced in the inferior/superior parietal and occipital cortices in PD patients with autonomic failure[20], in agreement with the negative correlation reported between intellectual impairment in PD and rCMRglc in posterior association regions such as the bilateral parietal and occipital gyri[21]. Both studies provided early indications that cortical hypometabolism may be primarily associated with cognitive dysfunction in PD. It was also found that the relative metabolic activity in typically affected cortical regions was significantly correlated with scores for cognition, but not with those for motor performance and behavior in a combined cohort of PD patients without and with dementia[22]. This measure gave a high sensitivity and specificity of 0.91 and 1.00 for an ultimate clinical diagnosis of dementia. Indeed, we found that worsening executive dysfunction in non-demented PD patients is related bilaterally with lower rCMRglc in parieto-occipital association regions, and with higher rCMRglc in the cerebellum (Fig. 2). Extensive areas of hypometabolism are also evident in the posterior cortical regions, including the temporo-parieto-occipital, medial parietal, and inferior temporal cortices in PD patients with mild cognitive impairment[18]. These results support the notion that posterior cortical dysfunction is the primary imaging feature of cognitively-impaired PD patients at risk for developing dementia.

Cerebral Blood Flow Studies

Owing to the short half-life of the radiotracer, H_2O PET has been primarily used in brain activation studies to examine physiological processes underlying motor execution and learning[23, 24]. Nevertheless, this method has also been used to map rCBF alterations in PD patients at rest. Both rCBF and rCMRglc data measured with PET yield similar patterns of subcortical hyperactivity and cortical hypoactivity in PD patients; these are highly comparable to those from resting-state rCBF studies using SPECT perfusion data. For example, one study compared parametric maps of globally normalized rCBF in PD patients and age-matched normal volunteers using SPECT with 99mTc-ethyl cysteinate dimer (ECD)[25]. In patients with early-stage PD, rCBF increased in the bilateral putamen and the right hippocampus relative to controls. In patients with late-stage PD, rCBF increased in the bilateral putamen, pallidum, hippocampus, and cerebellum, the left ventrolateral thalamus, and the right insula and inferior temporal cortex. Thus, significant rCBF changes in PD are associated with the pathophysiology and progression in the functional architecture of thalamocortico-basal ganglia circuits and related pathways.

By contrast, rCBF declines in the supplementary motor area (SMA) and the dorsolateral prefrontal cortex (DLPFC) in PD patients using SPECT with 99mTc-hexamethyl propylene amine oxime (HMPAO)[26]. In a subgroup of patients with Hoehn-Yahr III/IV, rCBF decreased in the SMA, and in the DLPFC and insular cortex. The degree of rCBF decline in the DLPFC or the insular cortex was correlated with UPDRS motor scores. rCBF was also significantly reduced in the bilateral posterior parietal and occipital cortices in non-demented PD patients relative to normal individuals using SPECT with N-isopropyl-p-[^{123}I]iodoamphetamine (IMP)[27]. There was a strong positive correlation between the scores in a visual-processing task and rCBF in the right visual association area in PD patients. This work demonstrates that posterior parietal and occipital hypoperfusion is a consistent feature in non-demented PD patients and the latter is likely to underlie impaired visual cognition.

SPECT perfusion data have proven useful for characterizing the unique features of cortical hypoperfusion in PD with dementia. Previous studies in patients with Hoehn-Yahr III–IV PD showed significant rCBF decreases in the left frontal/parietal association cortices with IMP[28] and in the precuneus and inferior parietal regions with HMPAO[29], consistent with the impaired visuospatial perception in demented PD. Furthermore, temporal and more extensive parietal hypoperfusion are often seen in demented patients[30]. The cortical hypoperfusion might be clinically useful in discriminating PD patients with dementia from those without cognitive impairment.

In summary, imaging studies of brain metabolism and perfusion have revealed unique and comparable pathological features underlying varying degrees of motor and cognitive dysfunction in patients with PD. The characteristic patterns of abnormal regional cerebral metabolism and perfusion are to a large degree independent of global measures of brain activity in non-demented patients with PD as described previously[3, 31]. The generally similar findings from these two imaging measures of brain function indicate close coupling between cerebral blood flow and metabolism in PD under resting conditions. These results

have established molecular-functional-clinical correlates of the impaired cortico-subcortical circuitry in PD.

Functional Brain Imaging: Multivariate Analyses

The measurements of local metabolic rates or blood flow changes may not fully account for the complex nature of brain networks involved in neurodegenerative processes and their modulation by therapy. These processes may be better represented by spatial covariance patterns among spatially distributed functional regions that can be altered by the presence of disease or behavioral activation. Many computing methods have been used in the analysis of rCMRglc and rCBF data to compare groups in the same resting state[32–35] and under brain activation conditions[36–38]. The resultant topographic patterns describe functional connectivity and are commonly referred to as disease-specific brain networks.

Metabolic Network Analyses

We have developed a statistical modeling approach to detect and quantify regional functional interactions in neurodegenerative disorders[31, 39]. This method, known originally as the scaled subprofile model (SSM), uses PCA to identify regional covariance patterns using images from a combined group of patients and controls or a single group of individuals (software freely available at our website http://www.feinsteinneuroscience.org). These patterns reflect the covariation of increased or decreased activity in regional brain function in patients relative to the normal population or in relation to the correlation with a behavioral variable.

SSMPCA allows for the prospective quantification of covariance pattern expression in individual subjects. Subject scores computed from functional brain images can be correlated with clinical or physiological parameters on a single-case basis[3]. Of note, these scores have higher signal-to-noise ratios than decreasing levels of dopaminergic markers such as FDOPA or FPCIT with increasing disease severity. Thus, SSMPCA may offer greater sensitivity for detecting spatiotemporal changes in brain network activity during progression or following therapy.

Many imaging studies have been performed to implement and validate network methods for the diagnosis and evaluation of patients with PD and related movement disorders[39, 40]. Using SSMPCA analysis of FDG PET data we consistently revealed a pattern of regional metabolic covariation characterized by lentiform, thalamic, cerebellar, pontine, and sensorimotor hypermetabolism, along with hypometabolism in the lateral PMC, SMA, and parieto-occipital regions (Fig. 3). The subject scores for this PD-related covariance pattern (PDRP) are elevated in PD patients, and are correlated positively with clinical disease ratings and negatively with striatal FDOPA uptake or DAT binding[3, 41, 42]. This pattern has been confirmed in multiple cohorts of PD patients[43–45] and parkinsonian primates[46] scanned with different tomographs. In addition, PDRP expression showed an excellent test-retest reproducibility [intraclass correlation coefficient (ICC) >0.94] between FDG PET imaging sessions conducted OFF and ON medications in independent groups of PD patients at early and advanced stages[39]. Moreover, disease-specific covariance patterns for multiple system atrophy (MSA), progressive supranuclear palsy and parkinsonian tremor have also

been developed for more accurate differential diagnosis of PD from atypical parkinsonism on a single-case basis[45, 47–49].

SSMPCA analysis of FDG PET data can also reveal the specific networks associated with cognitive dysfunction in PD. By using this method in non-demented PD patients, we identified a covariance pattern that is correlated with memory and executive functioning[50]. This PD-related cognitive pattern (PDCP) is characterized by hypermetabolism in the cerebellar vermis and dentate nuclei and hypometabolism in frontal and parietal association areas (Fig. 4). Similar results have been reported from VOI-based SSMPCA analysis[51] and another multivariate method based on partial least squares[34]. PDCP activity predicted memory or visuospatial function, and perceptual motor speed in a prospective validation sample of PD patients of similar disease duration and severity. In addition, PDCP scores showed excellent test–retest reliability (ICC >0.89) in patients undergoing repeat FDG PET imaging OFF and ON medications. PDCP is orthogonal to PDRP as its expression is independent of UPDRS motor scores in individual PD patients.

Importantly, the topography of the PD-related metabolic covariance pattern identified in these studies is in line with experimental models of parkinsonism[3, 46]. Specifically, this supports the notion of enhanced pallido-thalamic inhibition as the main functional substrate of parkinsonian bradykinesia. The subject scores for PDRP correlate with objective disease severity ratings and with independent measures of nigrostriatal dopamine function. Furthermore, the PDRP scores and rCMRglc within key hypermetabolic regions obtained from preoperative FDG PET scans are related to neuronal firing rates in the GPi and STN measured during stereotaxic neurosurgery[52, 53]. On the contrary, the PDCP scores did not show such relationships despite their correlation with cognitive impairment in patients. This is further evidence that the PDRP is an indirect measure of an abnormal physiological signal resulting from hyperactivity in the basal ganglia-thalamic-motor cortical loop.

Blood Flow Network Analyses

PD-related brain network patterns based on SSMPCA can be directly identified and prospectively accessed by using rCBF images from PET or SPECT. VOI-based network analysis of ECD SPECT data from PD patients and age-matched healthy controls revealed a pattern characterized by relative increases in putaminal, thalamic, and cerebellar perfusion along with decreases in the frontal operculum and in the medial temporal cortex[54]. The subject scores for this PDRP pattern were significantly increased in PD patients relative to healthy control and MSA groups. These features agree very well with those reported in the PDRP derived from FDG PET images.

Notably, the PET-derived PDRP scores computed from ECD SPECT scans more accurately separate PD patients from normal controls and MSA patients[54, 55]. Receiver operating characteristic analysis indicated that the PDRP measures yielded an overall diagnostic accuracy of 0.91, with a sensitivity of 0.97 and specificity of 0.71 and 0.80 for distinguishing PD from the other two groups. Hence, the disease-related patterns identified with FDG PET can be reliably assessed in SPECT perfusion scans to discriminate between healthy controls and patients with PD and atypical parkinsonism.

The disease-related patterns seen in PDRP derived from FDG PET and ECD SPECT images are also similar to those revealed by another multivariate brain mapping method based on independent component analysis (ICA). A SPECT study compared differences in rCBF between PD patients and age-matched controls with SPM after decomposing the images into disease-related and unrelated components[33]. In the disease-related components, PD patients revealed significantly higher normalized rCBF in the putamen, pallidum, thalamus, brainstem, and cerebellum, and significant hypoperfusion in the parieto-temporo-occipital cortex, DLPFC, insula, and cingulate gyrus. Importantly, motor UPDRS scores in patients correlated negatively with rCBF in the insula and cingulate gyrus. The abnormal regions revealed by both ICA and PCA are consistent with the current model of parkinsonism.

We have validated the PDRP or PDCP network as a reliable measure of parkinsonism or cognitive dysfunction by computing its activity prospectively in H_2O and FDG PET scans from PD patients and healthy volunteers[56]. PDRP expression was significantly elevated in PD patients, using either H_2O or FDG PET scans. A significant correlation was present between PDRP/PDCP scores computed from H_2O and FDG images in the same cohort of PD patients. This relationship has established the clinical utility of network quantification with rCBF data in the early differential diagnosis of PD. For example, PDRP/PDCP scores were computed in a prospective cohort of normal controls and patients with early- and late-stage PD who underwent H_2O PET imaging. We found that PDRP scores performed better than those for PDCP in separating early PD from controls. This difference in PDRP and PDCP scores from cross-sectional data is in line with the observation from a longitudinal study of disease progression with FDG PET[42], indicating that the manifestation of motor symptoms precedes cognitive dysfunction in early PD.

The reliability of PDRP/PDCP expression computed in rCBF scans has also been evaluated within subjects using a test–retest design in mild and advanced PD patients[56]. These patients were scanned twice within one H_2O PET imaging session at baseline and during treatment with levodopa (LD) infusion or deep brain stimulation (DBS). PDRP/PDCP scores measured with rCBF data have very high reproducibility (ICC >0.92), comparable to that from rCMRglc data acquired between FDG PET sessions separated by up to 2 months. This high reproducibility is evident in both early-stage and advanced PD patients scanned at baseline and during treatment.

PDRP/PDCP expression can also be assessed prospectively with rCBF data acquired from arterial spin labeling (ASL) perfusion MRI. We have shown that ASL MRI is comparable to FDG PET in quantifying PDRP network activity in individual patients and healthy controls[57]. Indeed, the PDRP scores in PD patients measured concurrently with both rCBF and rCMRglc images were equally elevated from the controls and significantly correlated with each other. With further technical refinement this imaging modality has been successful in deriving analogous spatial covariance patterns associated with motor and cognitive dysfunction in PD[58].

In summary, the motor and cognitive symptoms of PD have been linked to abnormal spatial covariance patterns involving different aspects of the basal ganglia-thalamocortical pathways. These patterns closely resemble specific physiological and anatomical brain

networks known to be operating in disease states, and are highly reproducible across independent patient populations and tomographs at separate institutions. Individual subject scores for the motor-related topography are significantly elevated in PD patients and correlate with bradykinesia and rigidity ratings. In addition, subject scores for the cognition-related topography predict behavioral performance. Besides the use of FDG PET data, pattern derivation and prospective assessment can also be achieved with rCBF data obtained from PET and more routine SPECT methods as well as newly-developed MRI perfusion techniques.

Functional Neuroimaging in the Evaluation of Therapeutic Interventions

Reliable *in vivo* markers of neuronal activity are necessary to assess the medical or surgical outcome in PD. Currently available clinical rating scales are inherently variable and relatively insensitive, and may not accurately reflect the extent of therapy-mediated changes in regional brain function. Conversely, quantitative functional imaging markers of cerebral metabolism and blood flow in the resting state may serve as suitable outcome measures for the treatment of PD. These measures may help select patients for clinical trials by providing more accurate diagnosis on an individual case basis and may afford a useful tool in predicting clinical outcomes for certain neurosurgical interventions.

Effects of Dopaminergic Therapy on Brain Function

PET/SPECT has been used to quantify regional functional changes associated with successful drug therapy. We reported that LD infusion significantly decreased rCMRglc in the putamen, thalamus, cerebellum, and primary motor cortex, along with a significant decline in PDRP expression[59] (Fig. 5). Changes in pallidal metabolism and PDRP activity were negatively correlated with clinical improvement in UPDRS motor ratings. These confirmed that lentiform hypermetabolism or hyperfusion in PD may be in part reversible by LD[60]. The response to dopaminergic therapy in PD patients may be mediated by the modulation of cortico-striato-pallido-thalamocortical pathways.

PET has played a key role in unraveling the metabolic and neurovascular effects of LD therapy for PD. Both H_2O and FDG PET images have been used to quantify LD-mediated changes in the expression of motor- and cognition-related PD covariance patterns as well as in rCBF and rCMRglc in PD patients before and after intravenous LD infusion[61]. There was a significant dissociation between rCBF and rCMRglc in the modulation of the PDRP by LD treatment, characterized by decreases in network activity in the rCMRglc images but concurrent increases in the rCBF images. This treatment also induced decreases in rCMRglc and increases in rCBF in the putamen/pallidum, dorsal midbrain/pons, STN, and ventral thalamus. These are the same regions that exhibit increased brain activity in PD with either rCMRglc or rCBF data obtained off medication as described above. These results indicate that flow–metabolism dissociation is a unique feature of LD treatment. The elevations in rCBF and in the corresponding PDRP network activity may be attributed to a direct action of dopaminergic drugs on the microvasculature in the close proximity of monoaminergic terminals. This LD-mediated disassociation between blood flow and metabolism calls for great caution when interpreting rCBF findings in patients who have taken dopaminergic medications or undergone insufficient washout before imaging.

Stereotaxic Surgical Therapies

Neurosurgery can provide effective symptomatic relief in patients with advanced PD by performing localized interventions on several deep nuclei that serve as key relay stations within the basal-ganglia-cortical motor circuitry and related pathways. DBS at high frequency offers a reversible treatment for PD without the permanent side-effects caused by an ablative lesion. In addition, DBS parameters can be adjusted postoperatively for optimal clinical benefits on an individual basis. A number of subcortical targets have been stimulated to achieve long-term improvement in the motor and non-motor symptoms of PD[62–64], including mainly pallidal and subthalamic DBS to improve general motor features and ventral intermediate (Vim) thalamic DBS to suppress tremor.

Neuroimaging studies with rCMRglc and rCBF have shed important light on the therapeutic mechanisms underlying these procedures. Ipsilateral and contralateral changes in regional brain function can be detected in the PMC, SMC, SMA, and cerebellum using both FDG and H_2O PET following unilateral DBS at the internal and external parts of the globus pallidus[9, 65]. Interestingly, unilateral Vim DBS leads to rCBF decreases in the ipsilateral SMC and the contralateral cerebellum, as well as concurrent increases in the ipsilateral ventral thalamus[66]. Changes in tremor acceleration and rCBF are correlated in the ipsilateral cortical regions; changes in tremor frequency and rCBF are correlated in the contralateral cerebellum and pons. These results suggest that DBS delivers symptomatic relief by modulating the activity of cerebello-thalamocortical pathways.

Stimulation at the STN is considered to be more effective than at the GPi in improving PD symptoms by affecting more than one inhibitory output area of the basal ganglia, i.e. both the GPi and the substantia nigra pars reticulata. An FDG PET study showed that rCMRglc decreased in the left rostral cerebellum with STN-DBS, but increased in both lower thalami extending to the midbrain area and remotely in the right frontal, temporal, and parietal cortices[14]. These data demonstrate an activating effect of DBS on its target structures and suggest a central role of the STN in motor, association, limbic, and cerebellar-basal ganglia circuits.

FDG PET has proven to be useful for directly comparing the specific metabolic effects of different interventions. It has been reported that metabolism is reduced in the GPi and caudal midbrain but elevated in the posterior parietal region following STN stimulation and subthalamotomy[16]. While the metabolic decline in the GPi is greater with a lesion, the metabolic increase is greater with stimulation. PDRP expression is similarly reduced with both treatments. Moreover, we reported that both STN stimulation and LD therapy result in significant metabolic reductions in the putamen/pallidum, SMC, and cerebellar vermis, as well as elevations in the precuneus[67]. Reduction in the lentiform metabolism may reflect deactivation of the inhibitory basal ganglia output nuclei following suppression of the synaptic activity of STN projections. Comparable declines in PDRP activity have also been observed with both interventions (Fig. 5), and they are correlated with clinical improvement. This is in excellent agreement with the findings reported with FDG PET in subthalamotomy[68] and DBS at the GPi[9] and STN[69]. These results suggest that effective treatments for PD are facilitated by a common mechanism involving the modulation of pathological brain networks.

It is of interest to note that PDCP expression assessed by rCMRglc and rCBF scans in the same patients was not changed by symptomatic therapy with either intravenous LD infusion or STN-DBS[61]. Hence, PDCP assessment did not reveal any flow-metabolism disassociation evident with LD administration in PDRP noted above. These findings support the hypothesis that PDCP network activity is a reproducible imaging biomarker of cognitive function in PD and this measure may prove useful in clinical trials targeting the non-motor symptoms of PD.

H_2O PET has been used to measure resting rCBF responses to STN-DBS. Cerebral blood flow increases in the thalamus and midbrain, but declines bilaterally in premotor cortex[70]. Of note, significant correlations are present between improved rigidity and decreased rCBF in the SMA, between improved bradykinesia and increased rCBF in the thalamus, and between improved postural reflexes and decreased rCBF in the pedunculopontine nucleus (PPN). Increased rCBF in the thalamus and midbrain agrees with the rCMRglc results from FDG PET[14, 67]. These data indicate that STN stimulation appears to increase the firing of STN output neurons, which enhances inhibition of the thalamocortical projections, ultimately decreasing blood flow in cortical targets. Furthermore, blood flow increases bilaterally in the STN and in the left lentiform during bilateral STN DBS[71], but declines in the left SMA (BA 6), left ventrolateral thalamus, and right cerebellum. Changes in rCBF in the basal ganglia or the SMA and thalamus are both correlated with the improvement in motor function. STN DBS in resting patients may also result in deactivation of the thalamic anteroventral and ventrolateral nuclei and the SMA.

STN-DBS in PD has also been examined by measuring resting-state rCBF with SPECT. In patients with stable clinical improvement during a long-term follow-up study[72], STN-DBS at 5 months induced a reversible increase of rCBF in the pre-SMA, PMC, and DLPFC regions from the preoperative baseline. Blood flow increased further from 5 to 42 months in these frontal areas, and also in the primary sensorimotor cortices, pallidum, ventral lateral thalamus, cerebellum, pons, and midbrain, involving the substantia nigra. The improvement in motor scores was correlated with the rCBF increase in the pre-SMA and PMC. Long-term STN-DBS leads to progressive improvement in neural activity in the frontal motor/association areas, along with increased activity in subcortical structures in the later phase.

There are bound to be agreements and discrepancies across the many neuroimaging studies on the functional effects of STN-DBS. The major disagreement is likely to come from different neurosurgical protocols, imaging techniques, and analytical methods. The second difference may stem from varied and limited sample sizes, and the inhomogeneous clinical characteristics of PD patients included in the study. The third difference may be the use of rCBF or rCMRglc as an outcome measure for the therapeutic trial. Although STN stimulation results in similar changes in regional brain activity and PDRP expression whether in rCMRglc or rCBF scans, a small difference may still arise from the potential residual effects of dopaminergic medications on rCBF values across studies.

H_2O PET can also detect the rCBF activation patterns induced by STN-DBS under task conditions. One study disclosed that rCBF increases significantly in the SMA, cingulate cortex, and DLPFC with STN stimulation during a motor activation task[73]. This suggests

that STN DBS plays a role in enhancing non-primary motor cortical areas, especially the DLPFC showing greater activation than in the GPi during effective stimulation. Bilateral STN DBS worsened the performance of a fast-paced cognitive task of random number generation in PD[74]. Cerebral blood flow was reduced in the left dorsal and inferior frontal gyri, DLPFC, and the posterior and right anterior cingulate, but increased in the right GPi during the task. STN stimulation activates its output neurons to the GPi and significantly changes pallidal coupling with prefrontal, cingulate, and temporal cortices during the performance of a cognitive experiment.

It has been proposed that the axial symptoms in PD can be effectively improved by stimulation at the PPN. Cerebral blood flow was measured by H_2O PET at rest and during a self-paced motor task of the lower limbs in patients with advanced PD who were treated with unilateral PPN-DBS[75]. Stimulation induced significantly increased rCBF in subcortical regions such as the thalamus, cerebellum, and midbrain as well as in different cortical areas involving the medial SMC extending into the caudal SMA (BA 4/6). Some of these regions are similar to the H_2O PET observations during STN-DBS. An FDG PET study also demonstrated that PPN DBS can improve non-motor function in the cognitive domain as indicated by relative prefrontal and cingulate hypermetabolism and cerebellar hypometabolism[76]. It remains to be seen in a large sample how PPN-DBS affects the clinical correlates of regional brain function and whether it can modulate PDRP activity as evident in other interventions.

In summary, PET/SPECT imaging of rCMRglc and rCBF is a useful experimental method for assessing the modulation of structure/functional relationships during the successful treatment of PD. Treatment with LD or DBS surgery in patients with PD alters activity in the putamen, pallidum, thalamus, and cerebellum, and partly restores the physiological substrate in limbic and associative cortical regions of the basal ganglia. In addition, clinical improvement is correlated with the changes in regional brain activity as well as in the expression of a PD-related covariance pattern. These interventions are consistently associated with modulation of regional brain function and suppression of a specific functional network involving elements of the cortico-striato-pallido-thalamocortical and the cerebello-cortical motor loops.

Conclusion

PET/SPECT has been widely used to identify changes in regional cerebral glucose metabolism and blood flow in PD. The measurements of cerebral metabolism and perfusion provide unique information on the topography of widespread functional alterations in the brains of PD patients, which is not available from studies with presynaptic or postsynaptic dopaminergic radioligands. Much effort has been devoted to the development of novel analytical methods for the validation of brain networks in functional imaging data. Such spatial covariance patterns may afford clinically useful markers in the differential diagnosis of parkinsonism and in the evaluation of disease severity and therapeutic response. Many studies have established the specific roles of imaging in preoperative patient selection for clinical trials in parkinsonism. A major contribution in this line of research has been a complementary analytical approach using both voxel-wise brain mapping and network

modeling strategies to determine the relationships between localized functional abnormality and the expression of widely distributed brain networks. Applications of these techniques may provide greater insights into the pathophysiology of PD and offer more accurate assessment of the inherent functional changes that occur with disease onset, progression, and successful therapy.

Acknowledgments

This review was supported by NIH (R01 NS 35069) and the Morris K. Udall Center of Excellence for Parkinson's Disease Research (NIH P50 NS 071675) at The Feinstein Institute for Medical Research, USA.

References

1. Thobois S, Jahanshahi M, Pinto S, Frackowiak R, Limousin-Dowsey P. PET and SPECT functional imaging studies in Parkinsonian syndromes: from the lesion to its consequences. Neuroimage. 2004; 23:1–16. [PubMed: 15325346]
2. Peng S, Doudet DJ, Dhawan V, Ma Y. Dopamine PET imaging and Parkinson's disease. PET Clin. 2013; 8:469–485.
3. Ma Y, Tang C, Moeller JR, Eidelberg D. Abnormal regional brain function in Parkinson's disease: truth or fiction? Neuroimage. 2009; 45:260–266. [PubMed: 18992824]
4. Catalan MJ, Ishii K, Honda M, Samii A, Hallett M. A PET study of sequential finger movements of varying length in patients with Parkinson's disease. Brain. 1999; 122:483–495. [PubMed: 10094257]
5. Wichmann T, DeLong MR. Functional neuroanatomy of the basal ganglia in Parkinson's disease. Adv Neurol. 2003; 91:9–18. [PubMed: 12442660]
6. Braak H, Del Tredici K. Cortico-basal ganglia-cortical circuitry in Parkinson's disease reconsidered. Exp Neurol. 2008; 212:226–229. [PubMed: 18501351]
7. Brownell AL, Canales K, Chen YI, Jenkins BG, Owen C, Livni E, et al. Mapping of brain function after MPTP-induced neurotoxicity in a primate Parkinson's disease model. Neuroimage. 2003; 20:1064–1075. [PubMed: 14568476]
8. Guigoni C, Dovero S, Aubert I, Li Q, Bioulac BH, Bloch B, et al. Levodopa-induced dyskinesia in MPTP-treated macaques is not dependent on the extent and pattern of nigrostrial lesioning. Eur J Neurosci. 2005; 22:283–287. [PubMed: 16029219]
9. Fukuda M, Mentis MJ, Ma Y, Dhawan V, Antonini A, Lang AE, et al. Networks mediating the clinical effects of pallidal brain stimulation for Parkinson's disease: a PET study of resting-state glucose metabolism. Brain. 2001; 124:1601–1609. [PubMed: 11459751]
10. Eckert T, Barnes A, Dhawan V, Frucht S, Gordon MF, Feigin AS, et al. FDG PET in the differential diagnosis of parkinsonian disorders. Neuroimage. 2005; 26:912–921. [PubMed: 15955501]
11. Teune LK, Bartels AL, de Jong BM, Willemsen AT, Eshuis SA, de Vries JJ, et al. Typical cerebral metabolic patterns in neurodegenerative brain diseases. Mov Disord. 2010; 25:2395–2404. [PubMed: 20669302]
12. Powers WJ, Videen TO, Markham J, Black KJ, Golchin N, Perlmutter JS. Cerebral mitochondrial metabolism in early Parkinson's disease. J Cereb Blood Flow Metab. 2008; 28:1754–1760. [PubMed: 18575458]
13. Ghaemi M, Raethjen J, Hilker R, Rudolf J, Sobesky J, Deuschl G, et al. Monosymptomatic resting tremor and Parkinson's disease: a multitracer positron emission tomographic study. Mov Disord. 2002; 17:782–788. [PubMed: 12210876]
14. Hilker R, Voges J, Weisenbach S, Kalbe E, Burghaus L, Ghaemi M, et al. Subthalamic nucleus stimulation restores glucose metabolism in associative and limbic cortices and in cerebellum: evidence from a FDG-PET study in advanced Parkinson's disease. J Cereb Blood Flow Metab. 2004; 24:7–16. [PubMed: 14688612]

15. Lozza C, Marie RM, Baron JC. The metabolic substrates of bradykinesia and tremor in uncomplicated Parkinson's disease. Neuroimage. 2002; 17:688–699. [PubMed: 12377144]
16. Trost M, Su S, Su P, Yen RF, Tseng HM, Barnes A, et al. Network modulation by the subthalamic nucleus in the treatment of Parkinson's disease. Neuroimage. 2006; 31:301–307. [PubMed: 16466936]
17. Bohnen NI, Minoshima S, Giordani B, Frey KA, Kuhl DE. Motor correlates of occipital glucose hypometabolism in Parkinson's disease without dementia. Neurology. 1999; 52:541–546. [PubMed: 10025784]
18. Hosokai Y, Nishio Y, Hirayama K, Takeda A, Ishioka T, Sawada Y, et al. Distinct patterns of regional cerebral glucose metabolism in Parkinson's disease with and without mild cognitive impairment. Mov Disord. 2009; 24:854–862. [PubMed: 19199357]
19. Berti V, Polito C, Ramat S, Vanzi E, De Cristofaro MT, Pellicano G, et al. Brain metabolic correlates of dopaminergic degeneration in de novo idiopathic Parkinson's disease. Eur J Nucl Med Mol Imaging. 2010; 37:537–544. [PubMed: 19727712]
20. Arahata Y, Hirayama M, Ieda T, Koike Y, Kato T, Tadokoro M, et al. Parieto-occipital glucose hypometabolism in Parkinson's disease with autonomic failure. J Neurol Sci. 1999; 163:119–126. [PubMed: 10371072]
21. Wu JC, Iacono R, Ayman M, Salmon E, Lin SD, Carlson J, et al. Correlation of intellectual impairment in Parkinson's disease with FDG PET scan. Neuroreport. 2000; 11:2139–2144. [PubMed: 10923659]
22. Liepelt I, Reimold M, Maetzler W, Godau J, Reischl G, Gaenslen A, et al. Cortical hypometabolism assessed by a metabolic ratio in Parkinson's disease primarily reflects cognitive deterioration-[18F]FDG-PET. Mov Disord. 2009; 24:1504–1511. [PubMed: 19489069]
23. Boecker H, Ceballos-Baumann A, Bartenstein P, Weindl A, Siebner HR, Fassbender T, et al. Sensory processing in Parkinson's and Huntington's disease: investigations with 3D H(2)(15)O-PET. Brain. 1999; 122:1651–1665. [PubMed: 10468505]
24. Fukuda M, Mentis M, Ghilardi MF, Dhawan V, Antonini A, Hammerstad J, et al. Functional correlates of pallidal stimulation for Parkinson's disease. Ann Neurol. 2001; 49:155–164. [PubMed: 11220735]
25. Imon Y, Matsuda H, Ogawa M, Kogure D, Sunohara N. SPECT image analysis using statistical parametric mapping in patients with Parkinson's disease. J Nucl Med. 1999; 40:1583–1589. [PubMed: 10520695]
26. Kikuchi A, Takeda A, Kimpara T, Nakagawa M, Kawashima R, Sugiura M, et al. Hypoperfusion in the supplementary motor area, dorsolateral prefrontal cortex and insular cortex in Parkinson's disease. J Neurol Sci. 2001; 193:29–36. [PubMed: 11718747]
27. Abe Y, Kachi T, Kato T, Arahata Y, Yamada T, Washimi Y, et al. Occipital hypoperfusion in Parkinson's disease without dementia: correlation to impaired cortical visual processing. J Neurol Neurosurg Psychiatry. 2003; 74:419–422. [PubMed: 12640053]
28. Matsui H, Nishinaka K, Oda M, Hara N, Komatsu K, Kubori T, et al. Heterogeneous factors in dementia with Parkinson's disease: IMP-SPECT study. Parkinsonism Relat Disord. 2007; 13:174–181. [PubMed: 17145197]
29. Firbank MJ, Colloby SJ, Burn DJ, McKeith IG, O'Brien JT. Regional cerebral blood flow in Parkinson's disease with and without dementia. Neuroimage. 2003; 20:1309–1319. [PubMed: 14568499]
30. Osaki Y, Morita Y, Fukumoto M, Akagi N, Yoshida S, Doi Y. Three-dimensional stereotactic surface projection SPECT analysis in Parkinson's disease with and without dementia. Mov Disord. 2005; 20:999–1005. [PubMed: 15806567]
31. Spetsieris PG, Eidelberg D. Scaled subprofile modeling of resting state imaging data in Parkinson's disease: methodological issues. Neuroimage. 2011; 54:2899–2914. [PubMed: 20969965]
32. Moeller JR, Ishikawa T, Dhawan V, Spetsieris P, Mandel F, Alexander GE, et al. The metabolic topography of normal aging. J Cereb Blood Flow Metab. 1996; 16:385–398. [PubMed: 8621743]

33. Hsu JL, Jung TP, Hsu CY, Hsu WC, Chen YK, Duann JR, et al. Regional CBF changes in Parkinson's disease: a correlation with motor dysfunction. Eur J Nucl Med Mol Imaging. 2007; 34:1458–1466. [PubMed: 17437108]
34. Mentis MJ, McIntosh AR, Perrine K, Dhawan V, Berlin B, Feigin A, et al. Relationships among the metabolic patterns that correlate with mnemonic, visuospatial, and mood symptoms in Parkinson's disease. Am J Psychiatry. 2002; 159:746–754. [PubMed: 11986127]
35. Chen K, Reiman EM, Huan Z, Caselli RJ, Bandy D, Ayutyanont N, et al. Linking functional and structural brain images with multivariate network analyses: a novel application of the partial least square method. Neuroimage. 2009; 47:602–610. [PubMed: 19393744]
36. Friston KJ, Holmes A, Poline JB, Price CJ, Frith CD. Detecting activations in PET and fMRI: levels of inference and power. Neuroimage. 1996; 4:223–235. [PubMed: 9345513]
37. McIntosh AR, Bookstein FL, Haxby JV, Grady CL. Spatial pattern analysis of functional brain images using partial least squares. Neuroimage. 1996; 3:143–157. [PubMed: 9345485]
38. Carbon M, Eidelberg D. Function al imaging of sequence learning in Parkinson's disease. J Neurol Sci. 2006; 248:72–77. [PubMed: 16753182]
39. Ma Y, Tang C, Spetsieris PG, Dhawan V, Eidelberg D. Abnormal metabolic network activity in Parkinson's disease: test-retest reproducibility. J Cereb Blood Flow Metab. 2007; 27:597–605. [PubMed: 16804550]
40. Niethammer M, Eidelberg D. Metabolic brain networks in translational neurology: Concepts and Applications. Ann Neurol. 2012
41. Kaasinen V, Maguire RP, Hundemer HP, Leenders KL. Corticostriatal covariance patterns of 6-[18F]fluoro-L-dopa and [18F]fluorodeoxyglucose PET in Parkinson's disease. J Neurol. 2006; 253:340–348. [PubMed: 16222426]
42. Huang C, Tang C, Feigin A, Lesser M, Ma Y, Pourfar M, et al. Changes in network activity with the progression of Parkinson's disease. Brain. 2007; 130:1834–1846. [PubMed: 17470495]
43. Moeller JR, Nakamura T, Mentis MJ, Dhawan V, Spetsieres P, Antonini A, et al. Reproducibility of Regional Metabolic Covariance Patterns: Comparison of Four Populations. Journal of Nuclear Medicine. 1999; 40:1264–1269. [PubMed: 10450676]
44. Wu P, Wang J, Peng S, Ma Y, Zhang H, Guan Y, et al. Metabolic brain network in the Chinese patients with Parkinson's disease based on 18F-FDG PET imaging. Parkinsonism Relat Disord. 2013; 19:622–627. [PubMed: 23529021]
45. Teune LK, Renken RJ, Mudali D, De Jong BM, Dierckx RA, Roerdink JB, et al. Validation of parkinsonian disease-related metabolic brain patterns. Mov Disord. 2013; 28:547–551. [PubMed: 23483593]
46. Ma Y, Peng S, Spetsieris PG, Sossi V, Eidelberg D, Doudet DJ. Abnormal metabolic brain networks in a nonhuman primate model of parkinsonism. J Cereb Blood Flow Metab. 2012; 32:633–642. [PubMed: 22126913]
47. Eckert T, Tang C, Ma Y, Brown N, Lin T, Frucht S, et al. Abnormal metabolic networks in atypical parkinsonism. Mov Disord. 2008; 23:727–733. [PubMed: 18186116]
48. Poston KL, Tang CC, Eckert T, Dhawan V, Frucht S, Vonsattel JP, et al. Network correlates of disease severity in multiple system atrophy. Neurology. 2012; 78:1237–1244. [PubMed: 22491861]
49. Mure H, Hirano S, Tang CC, Isaias IU, Antonini A, Ma Y, et al. Parkinson's disease tremor-related metabolic network: characterization, progression, and treatment effects. Neuroimage. 2011; 54:1244–1253. [PubMed: 20851193]
50. Huang C, Mattis P, Tang C, Perrine K, Carbon M, Eidelberg D. Metabolic brain networks associated with cognitive function in Parkinson's disease. Neuroimage. 2007; 34:714–723. [PubMed: 17113310]
51. Lozza C, Baron JC, Eidelberg D, Mentis MJ, Carbon M, Marie RM. Executive processes in Parkinson's disease: FDG-PET and network analysis. Hum Brain Mapp. 2004; 22:236–245. [PubMed: 15195290]
52. Eidelberg D, Moeller JR, Kazumata K, Antonini A, Sterio D, Dhawan V, et al. Metabolic correlates of pallidal neuronal activity in Parkinson's disease. Brain. 1997; 120:1315–1324. [PubMed: 9278625]

53. Lin TP, Carbon M, Tang C, Mogilner AY, Sterio D, Beric A, et al. Metabolic correlates of subthalamic nucleus activity in Parkinson's disease. Brain. 2008; 131:1373–1380. [PubMed: 18400841]
54. Feigin A, Antonini A, Fukuda M, De Notaris R, Benti R, Pezzoli G, et al. Tc-99m ethylene cysteinate dimer SPECT in the differential diagnosis of parkinsonism. Mov Disord. 2002; 17:1265–1270. [PubMed: 12465066]
55. Eckert T, Van Laere K, Tang C, Lewis DE, Edwards C, Santens P, et al. Quantification of Parkinson's disease-related network expression with ECD SPECT. Eur J Nucl Med Mol Imaging. 2007; 34:496–501. [PubMed: 17096095]
56. Ma Y, Eidelberg D. Functional imaging of cerebral blood flow and glucose metabolism in Parkinson's disease and Huntington's disease. Mol Imaging Biol. 2007; 9:223–233. [PubMed: 17334854]
57. Ma Y, Huang C, Dyke JP, Pan H, Alsop D, Feigin A, et al. Parkinson's disease spatial covariance pattern: noninvasive quantification with perfusion MRI. J Cereb Blood Flow Metab. 2010; 30:505–509. [PubMed: 20051975]
58. Melzer TR, Watts R, MacAskill MR, Pearson JF, Rueger S, Pitcher TL, et al. Arterial spin labelling reveals an abnormal cerebral perfusion pattern in Parkinson's disease. Brain. 2011; 134:845–855. [PubMed: 21310726]
59. Feigin A, Fukuda M, Dhawan V, Przedborski S, Jackson-Lewis V, Mentis MJ, et al. Metabolic correlates of levodopa response in Parkinson's disease. Neurology. 2001; 57:2083–2088. [PubMed: 11739830]
60. Hilker R, Voges J, Thiel A, Ghaemi M, Herholz K, Sturm V, et al. Deep brain stimulation of the subthalamic nucleus versus levodopa challenge in Parkinson's disease: measuring the on- and off-conditions with FDG-PET. J Neural Transm. 2002; 109:1257–1264. [PubMed: 12373559]
61. Hirano S, Asanuma K, Ma Y, Tang C, Feigin A, Dhawan V, et al. Dissociation of metabolic and neurovascular responses to levodopa in the treatment of Parkinson's disease. J Neurosci. 2008; 28:4201–4209. [PubMed: 18417699]
62. Krack P, Batir A, Van Blercom N, Chabardes S, Fraix V, Ardouin C, et al. Five-year follow-up of bilateral stimulation of the subthalamic nucleus in advanced Parkinson's disease. The New England journal of medicine. 2003; 349:1925–1934. [PubMed: 14614167]
63. Follett KA, Weaver FM, Stern M, Hur K, Harris CL, Luo P, et al. Pallidal versus subthalamic deep-brain stimulation for Parkinson's disease. N Engl J Med. 2010; 362:2077–2091. [PubMed: 20519680]
64. Fasano A, Daniele A, Albanese A. Treatment of motor and non-motor features of Parkinson's disease with deep brain stimulation. Lancet Neurol. 2012; 11:429–442. [PubMed: 22516078]
65. Payoux P, Remy P, Miloudi M, Houeto JL, Stadler C, Bejjani BP, et al. Contrasting changes in cortical activation induced by acute high-frequency stimulation within the globus pallidus in Parkinson's disease. J Cereb Blood Flow Metab. 2009; 29:235–243. [PubMed: 18781162]
66. Fukuda M, Barnes A, Simon ES, Holmes A, Dhawan V, Giladi N, et al. Thalamic stimulation for parkinsonian tremor: correlation between regional cerebral blood flow and physiological tremor characteristics. Neuroimage. 2004; 21:608–615. [PubMed: 14980563]
67. Asanuma K, Tang C, Ma Y, Dhawan V, Mattis P, Edwards C, et al. Network modulation in the treatment of Parkinson's disease. Brain. 2006; 129:2667–2678. [PubMed: 16844713]
68. Trost M, Su PC, Barnes A, Su SL, Yen RF, Tseng HM, et al. Evolving metabolic changes during the first postoperative year after subthalamotomy. J Neurosurg. 2003; 99:872–878. [PubMed: 14609167]
69. Wang J, Ma Y, Huang Z, Sun B, Guan Y, Zuo C. Modulation of metabolic brain function by bilateral subthalamic nucleus stimulation in the treatment of Parkinson's disease. J Neurol. 2010; 257:72–78. [PubMed: 19662326]
70. Karimi M, Golchin N, Tabbal SD, Hershey T, Videen TO, Wu J, et al. Subthalamic nucleus stimulation-induced regional blood flow responses correlate with improvement of motor signs in Parkinson disease. Brain. 2008; 131:2710–2719. [PubMed: 18697909]

71. Geday J, Ostergaard K, Johnsen E, Gjedde A. STN-stimulation in Parkinson's disease restores striatal inhibition of thalamocortical projection. Hum Brain Mapp. 2009; 30:112–121. [PubMed: 18041743]

72. Sestini S, Ramat S, Formiconi AR, Ammannati F, Sorbi S, Pupi A. Brain networks underlying the clinical effects of long-term subthalamic stimulation for Parkinson's disease: a 4-year follow-up study with rCBF SPECT. J Nucl Med. 2005; 46:1444–1454. [PubMed: 16157526]

73. Limousin P, Greene J, Pollak P, Rothwell J, Benabid AL, Frackowiak R. Changes in cerebral activity pattern due to subthalamic nucleus or internal pallidum stimulation in Parkinson's disease. Ann Neurol. 1997; 42:283–291. [PubMed: 9307248]

74. Thobois S, Hotton GR, Pinto S, Wilkinson L, Limousin-Dowsey P, Brooks DJ, et al. STN stimulation alters pallidal-frontal coupling during response selection under competition. J Cereb Blood Flow Metab. 2007; 27:1173–1184. [PubMed: 17119543]

75. Ballanger B, Lozano AM, Moro E, van Eimeren T, Hamani C, Chen R, et al. Cerebral blood flow changes induced by pedunculopontine nucleus stimulation in patients with advanced Parkinson's disease: A [(15)O] H(2)O PET study. Hum Brain Mapp. 2009; 30:3901–3909. [PubMed: 19479730]

76. Alessandro S, Ceravolo R, Brusa L, Pierantozzi M, Costa A, Galati S, et al. Non-motor functions in parkinsonian patients implanted in the pedunculopontine nucleus: focus on sleep and cognitive domains. J Neurol Sci. 2010; 289:44–48. [PubMed: 19765737]

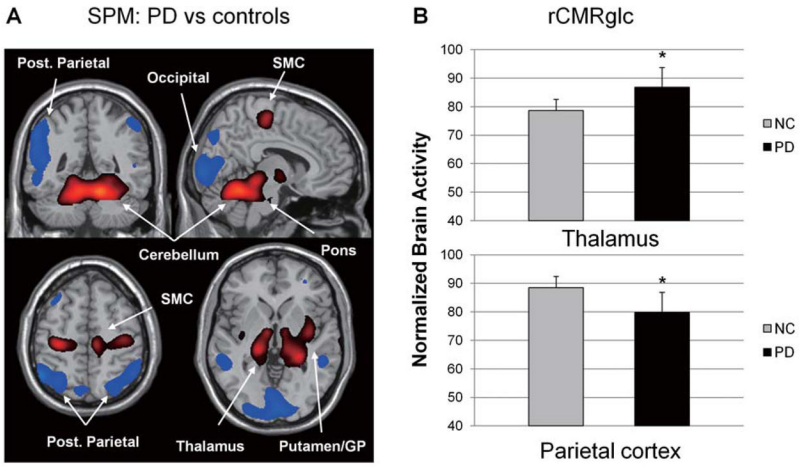

Fig. 1.

A: Brain regions with significant metabolic abnormality identified by SPM analysis of resting-state FDG PET scans in patients with Parkinson's disease (PD) and age-matched normal volunteers. PD patients showed relative metabolic increases (red) in the putamen/globus pallidus (GP) and thalamus, in the cerebellum and pons, and in the sensorimotor cortex (SMC), along with metabolic decreases (blue) in the parieto-occipital association areas. B: Bar diagrams (mean ± standard error) illustrating increased metabolic activity in the subcortical area and decreased activity in the cortex using rCMRglc data (P <0.01) that compared the PD patients to the controls. (Produced by the authors using FDG PET images described by Ma *et al.* J Cereb Blood Flow Metab 2007[39]. The display shows *t*-maps that are significant at P <0.001. The regional brain activity values were obtained *post-hoc* with a spherical VOI 8 mm in diameter centered at the peak of significant SPM clusters.)

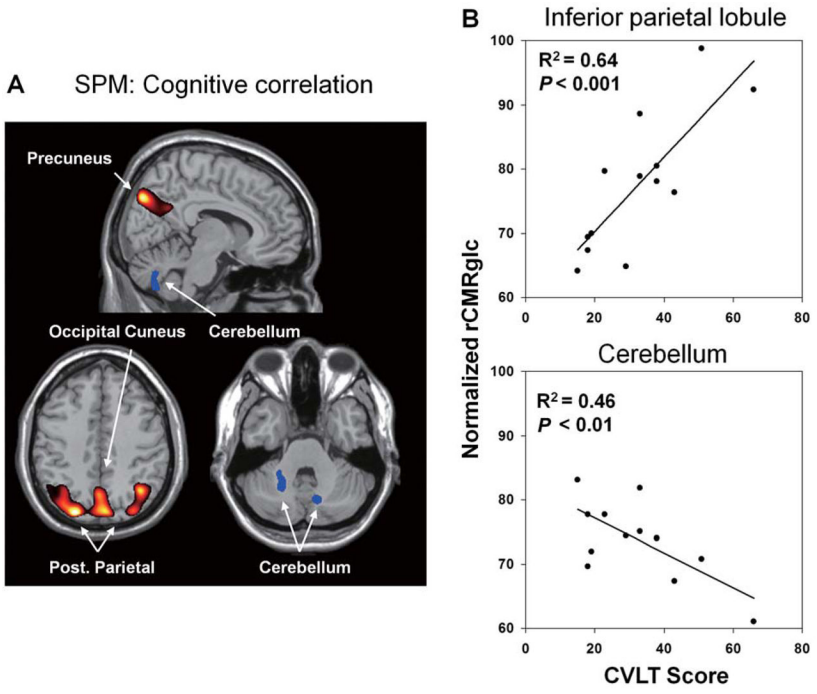

Fig. 2.

A: Brain regions with significant behavioral correlations identified by SPM regression analysis of resting-state FDG PET scans in non-demented patients with Parkinson's disease (PD). Scores on the California verbal learning test (CVLT) were positively correlated with metabolic activity in the precuneus and bilateral parieto-occipital association areas (red), and negatively with metabolic activity in the right brainstem and bilateral cerebellum (blue). B: Scatter plots illustrating significant linear relationships between the measure of cognitive dysfunction in PD with decreased brain activity in the parieto-occipital regions and increased brain activity in the cerebellum with rCMRglc data. Note that a lower CVLT score indicated a higher degree of cognitive dysfunction in individual patients. (Produced by the authors using FDG PET and clinical data described by Huang *et al.* NeuroImage 2007[50]. The display represents *t*-maps that are significant at $P < 0.01$. The regional metabolic values were obtained *post-hoc* with a spherical VOI 8 mm in diameter centered at the peak of significant SPM clusters.)

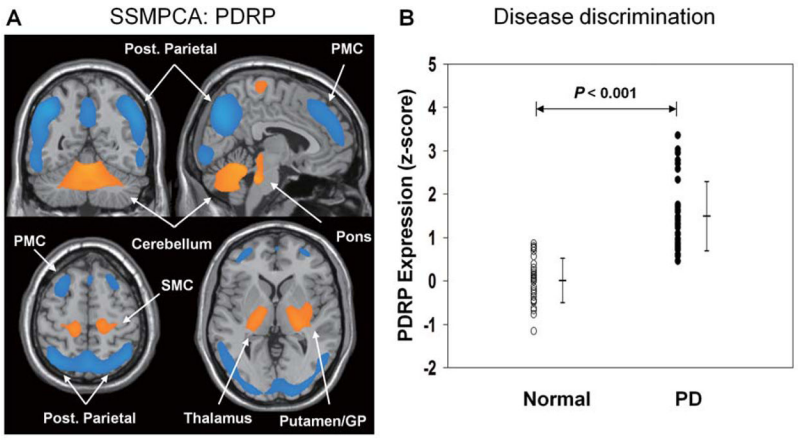

Fig. 3.

A: Parkinson's disease-related pattern (PDRP) identified by SSMPCA spatial covariance analysis of resting-state FDG PET scans in patients with Parkinson's disease (PD) and age-matched normal volunteers. This pattern was characterized by relatively increased metabolic activity (yellow) in the putamen/globus pallidus (GP) and thalamus, in the cerebellum and pons, and in the SMC. These changes covaried with relatively decreased metabolic activity (blue) in the lateral premotor cortex (PMC) and in the parieto-occipital association regions. B: Scatter plots of individual values and mean (± standard deviation) for PDRP expression in healthy controls (open circles) and PD patients (filled circles). PDRP network scores were significantly elevated in patients relative to controls. A higher PDRP score corresponded with more severe motor symptoms in individual patients. [Reproduced by the authors using FDG PET images described by Ma *et al.* J Cereb Blood Flow Metab 2007[39]. The display represents voxels that contributed significantly to the network at $P \leq 0.001$, and were demonstrated to be reliable ($P < 0.001$) on bootstrap estimation.]

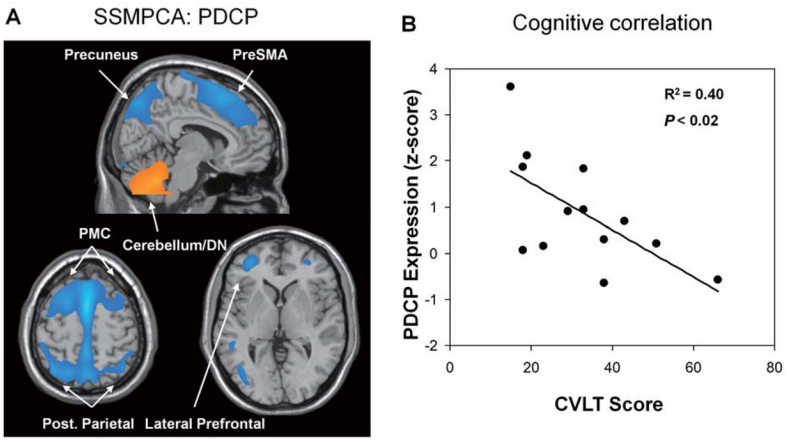

Fig. 4.

A: Parkinson's disease-related cognitive pattern (PDCP) identified by SSMPCA spatial covariance analysis of resting-state FDG PET scans in non-demented PD patients. This pattern was characterized by covarying metabolic reductions (blue) in the rostral supplementary motor area (pre-SMA) and precuneus, as well as in the dorsal premotor (PMC) and posterior parietal regions, and in the left prefrontal cortex. Relative metabolic increases (yellow) in the cerebellar vermis and dentate nuclei (DN) were also evident as part of this topography. B: Brain-behavioral correlations between PDCP network expression and neuropsychological performance in non-demented PD patients. There was a significant linear relationship between PDCP network activity and scores in the California verbal learning test (CVLT). Note that a lower CVLT score and higher PDCP activity indicated a greater degree of cognitive dysfunction in individual patients. (Reproduced by the authors using FDG PET and clinical data described by Huang *et al*. NeuroImage 2007[50].) The display represents regions that contributed significantly to the network at $P \leq 0.01$ and were demonstrated to be reliable ($P < 0.05$) by bootstrap estimation.

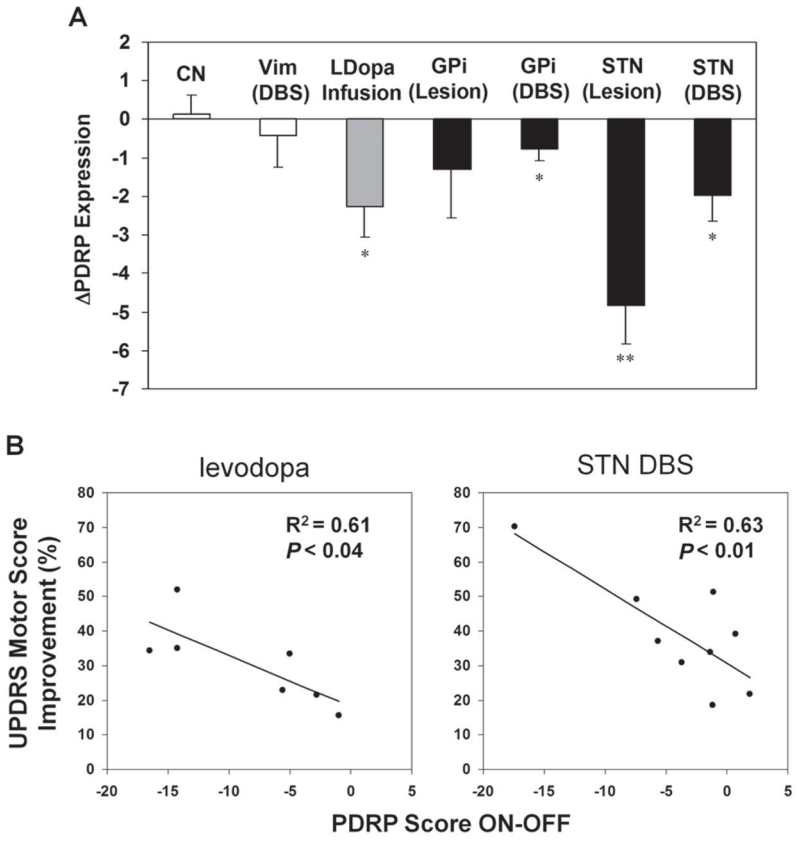

Fig. 5.

Network modulation and clinical correlation with antiparkinsonian interventions in patients assessed with FDG PET. A: Bar graph (mean ± SE) illustrating relative changes in the expression of the PD-related metabolic covariance pattern (PDRP) during antiparkinsonian therapy with LD infusion (shaded bar) and ventral pallidotomy, pallidal and STN DBS, and subthalamotomy (filled bars). Reduction in PDRP activity was greater in lesion *versus* DBS at the same target or in STN *versus* GPi by either lesion or DBS. For unilateral surgical intervention, PDRP reflected changes in network activity in the operated hemisphere. With LD infusion, the PDRP changes were averaged across hemispheres. CN, Control. B: Correlations between clinical improvement in UPDRS motor rating and treatment-mediated changes in PDRP activity. The clinical outcome in individual patients was significantly correlated with the degree of PDRP suppression following levodopa administration in mild PD patients and STN DBS in advanced PD patients. (Reproduced by the authors using FDG PET and clinical data described by Feigin *et al*. Neurology 2001[59] and Asanuma *et al*. Brain 2006[67]. $^{*}P$ <0.01; $^{**}P$ <0.005 *vs* untreated condition)